J Mater Sci (2011) 46:7228–7239
DOI 10.1007/s10853-011-5682-6

Ultrasonic sound speed analysis of hydrating calcium sulphate hemihydrate

A. C. J. de Korte · H. J. H. Brouwers

Received: 29 October 2010 / Accepted: 1 June 2011 / Published online: 28 June 2011

Abstract This article focuses on the hydration, and associated microstructure development, of β-hemihydrate to dihydrate (gypsum). The sound velocity is used to quantify the composition of the fresh slurry as well as the hardening and hardened—porous—material. Furthermore, an overview of available hydration kinetic and volumetric models for gypsum is addressed. The presented models predict the sound velocity through slurries and hardened products. These states correspond to the starting and ending times of the hydration process. The present research shows that a linear relation between the amount of hydration-product (gypsum) formed and sound velocity (Smith et al., J Eur Ceram Soc 22(12):1947, 2002) can be used to describe this process. To this end, the amount of hydration-product formed is determined using the equations of Schiller (J Appl Chem Biotechnol 24(7):379, 1974) for the hydration process and of Brouwers (A hydration model of Portland cement using the work of Powers and Brownyard, 2011) for the volume fractions of binder, water and hydration products during the hydration process.

Abbreviations

C	Volume fraction in water
c	Sound velocity
wbr	Water/binder ratio (m/m)

A. C. J. de Korte (✉)
Department of Civil Engineering, Faculty of Engineering Technology, University of Twente, P.O. Box 217, 7500 AE Enschede, The Netherlands
e-mail: a.c.j.dekorte@ctw.utwente.nl

H. J. H. Brouwers
Department of Architecture, Building and Planning, Eindhoven University of Technology, P.O. Box 513, 5600 MB Eindhoven, The Netherlands

Subscript

air	Air
DH	Di-hydrate (gypsum)
f	Fluid
HH	Hemihydrate
hp	Hardened product
s	Solid
sl	Slurry
t	Total
w	Water

Greek

α	Hydration degree
ρ	Specific density
ϕ	Volume fraction

Introduction

Currently, the hydration of hemihydrate to dihydrate and cement is studied by IR, SEM and Vicat techniques. Because the speed of hydration it is more difficult to measure the hydration curve and the different processes which take place. For the measurement of the hydration of cement and concrete, in the last decade, ultrasonic sound velocity measurements have been applied successfully [1–3]. This method has the advantage over the more traditional methods, such as the aforementioned Vicat-needle, SEM and IR, that ultrasonic measurements are continuous [4], and that they provide information about the microstructure development and the related properties like strength development [1]. Especially for hemihydrate hydration, due to the short hydration time, it is difficult to stop the hydration for discontinuous measurements. The ultrasonic sound velocity method used here is developed and patented by the University of Stuttgart [5].

The combining of ultrasonic measurements and volumetric composition has not been studied for hemihydrates yet, so far only studies are reported concerning cement paste and mortar, and also here these models were never combined to an overall volumetric composition model. Hence, this article will focus on the application of the ultrasonic sound velocity measurement for assessing the hydration curve of hemihydrate to gypsum. Therefore, it will be combined with information about the volume fractions of binders and hardened material during hydration and the classic hydration-time relations given by Schiller [6]. The currently used models do not fully combine this information, because either only focus on the microstructure development [7] or the effect of additives on the hydration [1, 2, 8]. In this article, a relation is established between ultrasonic speed and microstructure during hydration, from fresh state after mixing until hardened state at fully completed hydration.

Sound velocity of materials

This section describes the sound velocity through materials. Therefore, first a short introduction is given about sound velocity through fluid and non-porous material ('Introduction' section). Afterwards, the velocity through slurries ('Sound velocity of a slurry' section) and porous material ('Sound velocity of porous solid' section) is given. These two sections describe the starting and final states during the hydration, respectively.

Introduction

There are two methods to obtain the sound speed of the materials. The first method is the use of values from literature. Table 1 shows the sound speed through some materials. Besides this direct method, there is a second method to acquire the value of sound speed. This indirect method is based on the elastic modulus and density of the material and reads

$$c = \sqrt{\frac{K}{\rho}}, \tag{1}$$

with c the sound speed, K the bulk modulus and ρ the specific density. This method is suitable for fluids and gases, but it is not valid for solid materials. Since solid materials can support both longitudinal and shear waves, the shear modulus besides the bulk modulus influences the sound velocity. Therefore, the equation for solids read

$$c_{\text{long}} = \sqrt{\frac{K + \frac{4}{3}G}{\rho}}, \tag{2}$$

where K and G are the bulk and shear modulus of the solid, respectively, and ρ its specific density. Table 1 shows the elastic, bulk and shear modulus of several materials, as well as that of the fluids water and air. When applying Eqs. 1 and 2, the results for (non-porous) gypsum are 4289–4448 and 5019–5210 m/s, respectively. The results of both equations are lower than the experimental value of 6800 m/s provided by Losso and Viveiros [9]. This value is too high according to Y. Sakalli [Personal Communication, 2011].

Equations 1 and 2 tend to underestimate the sound velocity through solids. This is even more true for porous solids, which also contain voids. In 'Paste model for hydrating hemihydrate' section, the composition of a hemihydrates–water–gypsum system is addressed, used here for the development of a new model relating sound velocity and compositional properties.

Sound velocity of a slurry

This sub-section describes the sound velocity of a slurry, i.e. a suspension, containing entrapped air. Robeyst et al. [1] presented a model for ultrasonic velocity through fresh cement mixtures, based on the theoretical model of Harker and Temple [10] for ultrasonic propagation in colloids. According to these models, the effective wave velocity (c_e) in a suspension is given by:

$$c_e^2 = \left[\left(\phi_t \frac{1}{K_f} + (1-\phi_t)\frac{1}{K_s}\right) \times \left(\frac{\rho_f(\rho_s(\phi_t + (1-\phi_t)S) + \rho_f S\phi_t)}{\rho_s\phi_t^2 + \rho_f(S + \phi_t(1-\phi_t))}\right)\right]^{-1} \tag{3}$$

Table 1 Relevant physical properties of different materials; sound velocity of water, air, and steel according to [36]; sound velocity of gypsum according to [9]; elastic, bulk, and shear modulus and Poisson ratio according to [37–39]; bulk modulus air and water [39]

	Specific density (kg/m^3)	Sound speed (m/s)	Elastic modulus (GPa)	Bulk modulus (GPa)	Shear modulus (GPa)	Poisson ratio
Water	1000	1497		2.2		
Air		346		0.142		
Steel	7700	5930	170	79.3		
Dihydrate	2310	6800	45.7	42.5–45.7	15.7–17	0.33
Hemihydrate	2619		62.9	52.4	24.2	0.30
Anhydrite	2520		80	54.9	29.3	0.275

with the subscript 'f' referring to the fluid, 's' to the solid, and ϕ_t to the fluid volume fractions. The parameter S generally depends on the size and shape of the particles, the void fraction and the continuous phase viscosity [11], but it can be approximated by Eq. 4 for spherical particles in a fluid [12]

$$S = \frac{1}{2}\left(\frac{1+2(1-\phi_t)}{\phi_t}\right). \tag{4}$$

When also entrapped air is present in the fluid, the compressibility of the continuous phase can be corrected, assuming the air to be uniformly distributed

$$\frac{1}{K_f} = \left(1 - \frac{c_{air}}{\phi_t}\right)\frac{1}{K_{water}} + \frac{c_{air}}{\phi_t}\frac{1}{K_{air}}, \tag{5}$$

with c_{air} as the air volume fraction in the voids of the fluid and K_{air} the bulk modulus of air.

Sound velocity of porous solids

The equations from 'Introduction' section are not directly applicable to porous materials. Therefore, this subsection will describe two ways to calculate the sound velocity through porous material. 'Indirect method' section describes the indirect methods, in which the sound velocity is based on the bulk and shear modulus like in Eqs. 1 and 2. 'Direct method' section will focus on the direct methods, in which the calculations are based on the theoretical sound velocities of the non-porous materials as presented in Table 1.

Indirect method

When using the indirect method for calculation, the sound velocity through porous materials, the bulk modulus, shear modulus and density need to be computed. Analogue to thermal conductivity one could expect the boundaries for a material to be given by the parallel and series arrangement. Hoyos et al. [13] uses the parallel arrangement, this equation reads

$$K_e^{-1} = (1-\phi_t)K_s^{-1} + \phi_t K_f^{-1}, \tag{6}$$

with K_e the effective bulk modulus, K_s the bulk modulus of solid and K_f the bulk modulus of the fluid. The series equation reads

$$K_e = (1-\phi_t)K_s + \phi_t K_f. \tag{7}$$

The series arrangement can be used for the bulk and shear modulus. But using the parallel arrangement, the shear modulus (G_e) cannot be calculated since fluids do not have a shear modulus. In order to calculate the shear modulus, the relation between the bulk modulus and shear modulus [14] is as follows:

$$G_e = \frac{3K(1-2\upsilon)}{2(1+\upsilon)} \tag{8}$$

with ν the Poisson ratio of the solid. Arnold et al. [15] give the following equation for very porous media ($\phi_t > 0.4$) with spherical pores

$$K_e = K_s\frac{2(1-2\nu)(1-\phi_t)}{3(1-\nu)} \tag{9}$$

with K_s as the bulk modulus at zero void fraction and ν the poisson ratio at zero void fraction.

Besides a difference in bulk and shear modulus of a porous material, also the density will be different. The equation for effective density reads

$$\rho_e = (1-\phi_t)\rho_s + \phi_t p_f \tag{10}$$

with ρ_s and ρ_f as the density of the solid and the fluid, respectively.

Equations 6–10 can be used in Eqs. 1 and 2 to calculate the sound velocity of a porous material.

Summarizing, the combined equations for parallel arrangement without taking in account the contribution of the shear modulus read

$$c_e = \sqrt{\frac{K_s K_f}{(1-\phi_t)K_f + \phi_t K_s}\cdot\frac{1}{(1-\phi)\rho_s + \phi_t\rho_f}} \tag{11}$$

by combination of Eqs. 1, 6 and 10, for the series arrangement without shear modulus contribution, the sound velocity reads

$$c_e = \sqrt{\frac{K_s + \phi_t(K_f - K_s)}{\rho_s + \phi_t(\rho_f - \rho_s)}} \tag{12}$$

by combination of Eqs. 1, 7 and 10, for the bulk modulus according to Arnold et al. [15] the sound velocity reads

$$c_e = \sqrt{K_s\frac{(2-\upsilon)(1-\phi_t)}{3(1-\upsilon)}\cdot\frac{1}{(1-\phi_t)\rho_s + \phi_t\rho_f}} \tag{13}$$

by combination of Eqs. 1, 9 and 10, for the parallel arrangement with shear modulus according to Landau [14] the sound velocity reads

$$c_e = \sqrt{\frac{K_s K_f}{(1-\phi_t)K_f + \phi K_s}\cdot\frac{1}{(1-\phi_t)\rho_s + \phi_t\rho_f}\cdot\left(1+\frac{2(1-2\upsilon)}{(1+\upsilon)}\right)} \tag{14}$$

by combination of Eqs. 2, 6, 8 and 10, for the series arrangement with shear modulus according to Landau [14], the sound velocity reads

$$c_e = \sqrt{\frac{K_s + \phi_t(K_f - K_s)}{\rho_s + \phi_t(\rho_f - \rho_s)}\cdot\left(1+\frac{2(1-2\upsilon)}{(1+\upsilon)}\right)} \tag{15}$$

by combination of Eqs. 2, 7, 8 and 10, and for the bulk modulus according to Arnold et al. [15] with shear modulus according to Landau [14], the sound velocity reads

$$c_e = \sqrt{K_s \frac{(2-\upsilon)(1-\phi_t)}{3(1-\upsilon)} \cdot \frac{1}{(1-\phi_t)\rho_s + \phi_t \rho_f} \cdot \left(1 + \frac{2(1-2\upsilon)}{(1+\upsilon)}\right)} \tag{16}$$

by combination of Eqs. 2, 8, 9 and 10 with c_e as the effective sound speed, K_s and K_f the bulk modulus of the solid and the fluid, respectively, υ the poison ratio, ρ_s and ρ_f the specific density of the solid and the fluid, respectively, and ϕ_t the void fraction of the mixture. Equations 11–16 are applied and validated in 'Applying the volumetric models to sound velocity measurements' section.

Direct method

The sound velocity of a porous material can also calculated directly from the individual sound velocities of the individual phases. Roth et al. [16] used a simple equation to predict the effective sound speed in a porous medium. This equation reads

$$c_e = c_s(1-\phi_t) \tag{17}$$

with c_s the sound speed in the non-porous material and ϕ_t the void fraction. Dalui et al. [17] have added an exponent

$$c_e = c_s(1-\phi_t)^n \tag{18}$$

with exponent n being an empirical constant. For α-hemihydrate, Dalui et al. [17] proposed $n = 0.84$ and $c_s = 4571$ m/s.

A drawback of these empirical equations is that in the limit of the void fraction approaching unity, a sound velocity of zero is obtained, which is obviously not correct. Therefore, here an additional term is added to Eqs. 17 and 18 which takes into account the sound velocity of the fluid:

$$c_e = c_s(1-\phi_t) + c_f\phi_t \tag{19}$$

and

$$c_e = c_s(1-\phi_t)^n + c_f\phi_t^n \tag{20}$$

with c_f being the sound speed of the fluid. Equations 17–20 are based on a parallel arrangement. Another possibility is to use a series arrangement [18], and the equation for this arrangement reads

$$c_e = \frac{c_s c_f}{(1-\phi_t)c_f + \phi_t c_s} \tag{21}$$

with c_e as the effective velocity, c_s the velocity of the solid phase, c_f the velocity of the fluid and ϕ_t the void fraction.

Paste model for hydrating hemihydrate

In this section, a paste model for hydration of calcium sulphates is presented. This paste model is subsequently used for the calculation of the volume fractions of solids and voids in the slurry and solid materials. These volume fractions are needed for the calculation of the sound speed through porous media in following sections, since the void fraction influences the bulk and shear modulus as well as the density of the material, and hence the sound speed.

The model of Brouwers [19] is used to describe the volume fractions of binder, hardened product, water and shrinkage before, during and after hydration. This model makes use of the molar mass of the reactant and product as well as the reaction stoichiometry. It can be used for both α- and β-hemihydrate as well as anhydrite. The volume fractions read

$$\phi_{hp} = \frac{\alpha\left[\frac{v_c}{v_w} + \frac{w_n v_n}{v_w c}\right]}{\frac{v_c}{v_w} + \frac{w_0}{c_0}} \tag{22}$$

$$\phi_c = \frac{(1-\alpha)\left[\frac{v_c}{v_w}\right]}{\frac{v_c}{v_w} + \frac{w_0}{c_0}} \tag{23}$$

$$\phi_w = \frac{\frac{w_0}{c_0} - \alpha\left[\frac{w_n}{c}\right]}{\frac{v_c}{v_w} + \frac{w_0}{c_0}} \tag{24}$$

$$\phi_s = \frac{\alpha\left[1 - \frac{v_n}{v_w}\right]\frac{w_n}{c}}{\frac{v_c}{v_w} + \frac{w_0}{c_0}} \tag{25}$$

with ϕ_c, ϕ_{hp}, ϕ_w and ϕ_s as the volume fractions of binder, hardened product, water and shrinkage, respectively, and α the hydration degree, w_n/c the mass of non-evaporable water on mass of reacted hemihydrates, v_c/v_w the specific volume ratio of hemihydrate on water, w_n/c_0 the initial water/binder ratio and v_n/v_w the volume ratio of non-evaporable water on water. The values for w_n/c, v_c/v_w and v_n/v_w can be found in Brouwers [19] and Table 2. For $\alpha = 0$, Eqs. 22–25 give the volume fractions in case of a slurry of hemihydrate and water, while $\alpha = 1$ describes the case of the fully hydrated (porous) gypsum, so including its voids.

The total void fraction (ϕ_t) is the sum of the volume fraction of water and volume fraction of shrinkage, so the total void fraction is equal to

$$\phi_t = \phi_w + \phi_s = \frac{\frac{w_0}{c_0} - \alpha\frac{v_n}{v_w}\frac{w_n}{c}}{\frac{v_c}{v_w} + \frac{w_0}{c_0}}. \tag{26}$$

Table 2 Parameters of the paste model [19]

Substance	v_c/v_w	w_n/c	v_n/v_w	$v_n w_n/v_w c$	$V_s/v_w c$
$C\bar{S}(\gamma)$	0.39	0.265	0.60	0.16	0.106
$C\bar{S}H_{0.5}(\alpha)$	0.36	0.186	0.81	0.15	0.035
$C\bar{S}H_{0.5}(\beta)$	0.38	0.186	0.71	0.13	0.054

The void fraction before mixing corresponds to the water volume fraction of the slurry ($\alpha = 0$) and reads

$$\phi_t = \frac{\frac{w_0}{c_0}}{\frac{v_e}{v_w} + \frac{w_0}{c_0}}. \quad (27)$$

For a fully hydrated system ($\alpha = 1$), Eq. 26 yields

$$\phi_t = \frac{\frac{w_0}{c_0} - \frac{v_n}{v_w}\frac{w_n}{c}}{\frac{v_e}{v_w} + \frac{w_0}{c_0}}. \quad (28)$$

The void fraction of α-hemihydrate based dihydrate after full hydration ($\alpha = 1$), following Table 2, reads

$$\phi_t = \frac{\frac{w_0}{c_0} - 0.15}{0.36 + \frac{w_0}{c_0}}. \quad (29)$$

This equation was also introduced already by Schiller [20], which was also used by other researchers [17, 21]. Brouwers [19] and Yu and Brouwers [22] have compared experimental values with the model presented here, in particular Eq. 28, for hardened β-hemihydrate ($\alpha = 1$) and found good agreement.

Equations 23, 24 and 27 are applicable to the hydration of α- and β-hemihydrate, for $0 \leq \alpha \leq 1$, so not only for fully hydrated binder only. In the next sections, they will be applied to a hydrating system, so $0 < \alpha < 1$, measured using the ultrasonic velocity.

Hydration models

'Sound velocity of materials' section addressed the sound velocity of the material in the initial and final state of hydration. But besides these both states, also the process in between is interesting. Therefore, first a model for the relation between sound velocity and hydration degree is given. For the study of the hydration, the relation to time is essential, therefore hydration degree is related to time by use of analytical hydration models in 'Relation between hydration degree and time' section.

Relation between hydration degree and sound velocity

Smith et al. [23] describe the relation between hydration mechanism and ultrasonic measurements in aluminous cement. They provide a correlation between hydration degree and ultrasonic measurements. This correlation reads

$$\alpha = \frac{c_e - c_{sl}}{c_{hp} - c_{sl}} + \alpha_0, \quad (30)$$

with c_e is the measured sound velocity through mix, c_{sl} is the sound velocity at moment the velocity starts increasing (so, of the slurry), c_{hp} is the sound velocity when the velocity stops increasing (so, of the hardened product) and α_0 is the hydration degree at moment of c_{sl} (which is here zero). Equation 30 can be rewritten to

$$c_e = \alpha(c_{hp} - c_{sl}) + c_{sl}. \quad (31)$$

When it is invoked that at $\alpha = 0$ corresponds to $c_e = c_{sl}$ and at $\alpha = 1$ corresponds to $c_e = c_{hp}$.

Relation between hydration degree and time

In literature, several different analytical hydration models are introduced. Most models are based on the work of either Schiller [6, 24–26] or of Ridge and Surkevicius [27–29]. The equation of Schiller [6] has the advantage that it indirectly includes water/binder ratio in the parameters. The equation of Schiller [6] reads

$$t = K_1\sqrt[3]{\alpha} + K_2\left(1 - \sqrt[3]{1-\alpha}\right) + K_0, \quad (32)$$

in which K_0 equals the induction time (t_0). Schiller [6] emphasizes that K_1 and K_2 have clearly defined physical meanings and are not just fitting parameters.

Schiller [6] shows a number of simulations for the hydration of hemihydrate. In his simulations, K_1 is between 21 and 48.3 min and K_2 from 11 to 21.6 min. Beretka and van der Touw [30] used value for K_1 between 37.8 and 43.5 min and between 15.1 and 30.3 min for K_2 for a mixture with wbr of 0.70. Fujii and Kondo [31] used $K_1 = 44$ min and $K_2 = 276$ min for a wbr of 0.40. Although none of these authors specify the type of hemihydrate used, from the hydration time one can assume that it concerned α-hemihydrate. Singh and Middendorf [32] point out that the induction period for α-hemihydrate hydration is shorter than that for β-hemihydrate. But they also point out that β-hemihydrate hydrates faster because of its higher surface area which provides more nucleation sites for the crystallization of gypsum.

Experiments

Materials

Within this research, β-hemihydrate is used as the binder. The hemihydrate used during the experiments was produced from flue gas desulphurization gypsum, which is commonly used for the production of gypsum plasterboards. The particle size distribution (PSD) is shown in Fig. 1. The used β-hemihydrate consists of 94.5% pure hemihydrate, 3.9% limestone and 1.6% other compounds [22]. The hemihydrate has a Blaine value of 3,025 cm^2/g and a density of 2,619 kg/m^3. The Blaine value describes the fineness of the binder particle (hemihydrate). Hunger and Brouwers [33] point out that the Blaine test methods are not applicable for powders with higher fineness (i.e. particles <10 μm). The

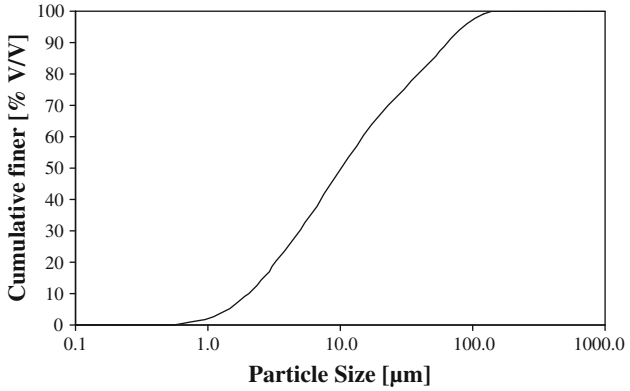

Fig. 1 Particle size distribution of applies hemihydrate

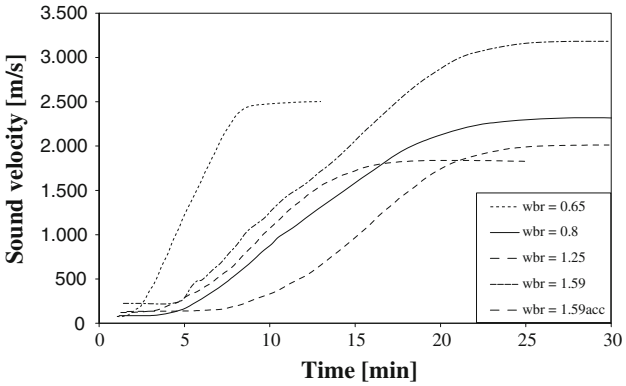

Fig. 2 Measured sound velocity by Grosse and Lehmann [35]

hemihydrates used has 50% of the particles smaller than 10 µm, therefore the Blaine value is less suitable. Another method to determine the fineness of powder is the use of specific surface area (SSA). Hunger [34] showed a method to calculate the specific surface area based on the PSD. Hunger and Brouwers [33] showed that there is a constant ratio between Blaine value and computed SSA. The Blaine value has to be multiplied by about 1.7 to obtain the SSA. Applied here, the SSA based on the given Blaine value would amount 5130 cm^2/g. The computation of the SSA using the PSD depends on the shape of the particles. For spheres, the shape factor equals unity. Using this shape factor, the SSA of the used hemihydrate would be 4432 cm^2/g. However, these powder particles are not spherical, and the amount of specific surface area is higher. To match computed SSA and Blaine value of 5130 cm^2/g, here a shape factor of 1.16 follows for the applied β-hemihydrate. It is noteworthy that Hunger and Brouwers [33] found shape-factor of 1.18 for α-hemihydrate.

Measurements

The measurements were executed in cooperation with the Materialprüfungsanstalt of the University of Stuttgart (Germany). The sound velocity of four water/binder ratios is measured during the experiments. The four water/binder ratios (wbr) are 0.63, 0.80, 1.25 and 1.59. Besides these four mixtures, also a mixture with wbr of 1.59 with 0.40% (m/m) accelerator is tested. Table 3 shows the mix-designs used during the experiments. Figure 2 shows the measured sound velocity during hydration of the four mixtures.

The hemihydrate hydration experiments with ultrasonic method were performed using the FreshCon system which was developed at the University of Stuttgart. The measurements are performed in a container, which consists of two polymethacrylate walls and u-shaped rubber foam element in the center, which are tied together by four screws with spacers. The volume of the mould is approximately 45 cm^3 for the test. The measurements were performed with use of two Panametrics V106, 2.25 MHz centre frequency sensors. For the processing of the measuring data during the experiments, in-house developed software (FRESHCON2) is used. More detailed information about the FreshCon system and the measurement procedure can be found in Reinhardt and Grosse [2].

The calculated void fractions of the mixtures in this research, based on the model of Brouwers [19], are given in Table 3 and shown in Fig. 3. Table 3 also shows the

Table 3 Mix designs, computed void fractions based on Brouwers [19] and the results of the ultrasonic measurements [35]

	Mix design				
	A	B	C	D	E
Water/hemihydrate ratio	0.63	0.8	1.25	1.59	1.59
Accelerator (m/m on hemihydrates)					0.40%
Before hydration					
Computed void fraction	0.624	0.678	0.767	0.807	0.807
Measured sound velocity (m/s)	75	85	134	223	134
After hydration					
Computed void fraction	0.493	0.566	0.685	0.740	0.740
Measured sound velocity (m/s)	2500	2300	2000	3172	1835

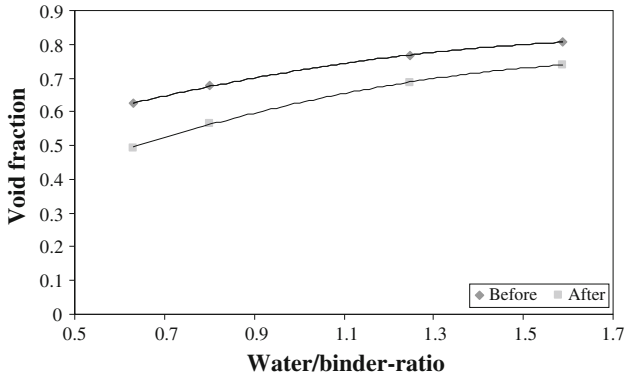

Fig. 3 Relation between water/binder ratio and computed void fraction based on Brouwers [19] before and after hydration

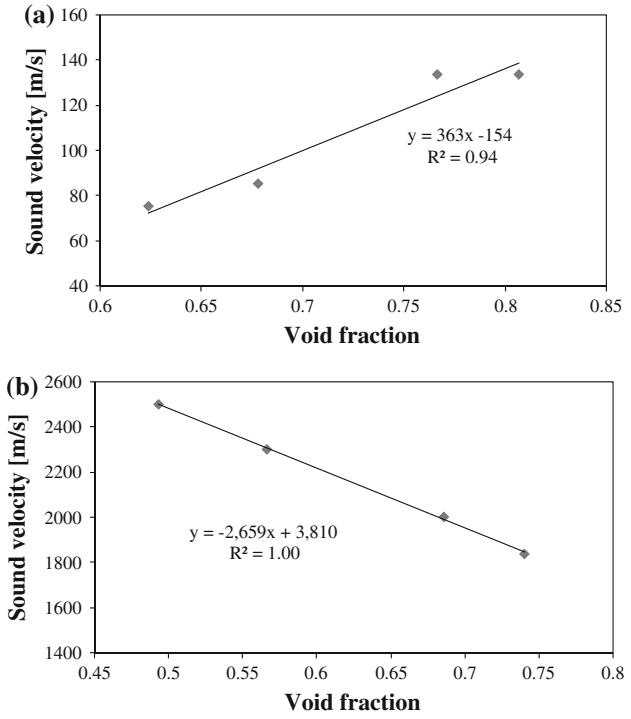

Fig. 4 Void fraction versus velocity **a** before hydration and **b** after hydration based on the experiments of Grosse and Lehmann [35]

measured ultrasonic velocity by Grosse and Lehmann [35]. Figure 4a and b is the graphic representations of the sound velocity data versus computed void fraction from Table 3. It can be noticed from the figures that there is a clear relation between void fraction and velocity as well before as after hydration, so $\alpha = 0$ and $\alpha = 1$, respectively. But the trend is exactly opposite before and after hydration. Before hydration, the velocity increases with increasing void fraction (i.e. water content), while the velocity is decreasing with increasing void fraction after hydration. In the next section, relations will be established between the volumetric composition (at $\alpha = 0$ and $\alpha = 1$) and sound velocity.

Applying the volumetric models to sound velocity measurements

Sound velocity through a slurry

Table 4 shows the results of Eq. 3 with $K_s = 52.4$ GPa, $K_f = 2.2$ GPa (Table 1). The calculated sound velocities with Eq. 3 are much higher than the measured sound velocity during the experiments. The main reason for this is the overestimation of the fluid bulk modulus as described by Robeyst et al. [1]. Therefore, the bulk modulus of the fluid is corrected with Eq. 5, with the bulk modulus of air 142 kPa and the bulk modulus of water 2.2 GPa (Table 1). Based on this equation, the air content (C_{air}) of the pore fluid can be derived, which is included in Table 4.

Further computations reveal that the volume fraction of air divided by the volume fraction of the binder in the slurry lies in a very small range (Table 4). This could indicate that air entered the slurry on the surface of the hemihydrate particles and a typical value is thus 2.7% (V/V) or 10 mL air per kg hemihydrate. Given the Blaine value of 3025 cm^2/g, this would mean 3.28×10^{-6} mL air per cm^2 hemihydrate surface ($= 3.28 \times 10^{-2}$ mL/m^2), corresponding to an air layer thickness of 32.8 nm.

Sound velocity of solid: indirect method

Table 5 shows the results of Eqs. 11–13 with $K_s = 44$ GPa, $K_f = 2.2$ GPa and $\nu = 0.33$ (Table 1). The use of bulk-modulus based on Eqs. 11 and 13 lead to an underestimation, while Eq. 12 leads to an overestimation of the velocity. Table 5 also shows the results for Eqs. 14–16. The best estimation of the sound velocity was found using Eq. 16. The difference between predicted values for this combination and experimental value becomes slightly larger when the water/binder ratio increases.

Table 4 Results of the slurry method Eq. 3 without entrapped air and derived air content with the use of the slurry method (Eqs. 3–5)

	Wbr	Initial void fraction	Measured velocity (m/s)	Computed velocity (Eq. 3)	Derived air content	
					C_{air} (%)	V_{air}/V_{HH} (%)
A	0.63	0.624	75	1520	1.69	2.85
B	0.8	0.678	85	1511	1.41	3.00
C	1.25	0.767	134	1503	0.63	2.09
D	1.59	0.807	223	1500	0.23	0.98
E	1.59^{acc}	0.807	134	1500	0.66	2.78

[acc] stands for 0.40% m/m accelerator added

Table 5 Results of the indirect method (Eqs. 11–16) and the direct method (Eqs. 17–21) with sound velocity (m/s), specific density (kg/m^3), bulk moduli (GPa), shear moduli (GPa), and poisson ratio (–) of gypsum taken from Table 1

	c_s (m/s)	A	B	C	D	E
Water/binder ratio		0.63	0.8	1.25	1.59	1.59
Accelerator						0.40%
Final void fraction		0.493	0.566	0.685	0.74	0.74
Measured		2500	2300	2000	3172	1835
Indirect method						
Eq. 11		1597	1545	1491	1476	1476
Eq. 12		3749	3601	3298	3122	3122
Eq. 13		2130	2029	1822	1699	1699
Eq. 14		1963	1899	1833	1815	1815
Eq. 15		4609	4427	4055	3838	3838
Eq. 16		2618	2495	2240	2089	2089
Direct method						
Eq. 17	6800	3448	2951	2142	1768	1768
Eq. 18	6800	3843	3373	2577	2193	2193
Eq. 18	4571	2584	2267	1732	1474	1474
Eq. 19	6800	4186	3799	3167	2876	2876
Eq. 20	6800	4670	4301	3666	3356	3356
Eq. 20	4571	3410	3195	2822	2637	2637
Eq. 21	6800	2476	2263	1985	1878	1878
Eq. 21	5440	2367	2184	1939	1845	1845
Eq. 21	4571	2271	2114	1899	1814	1814

Sound velocity of solid: direct method

The results of Eqs. 17–21 are shown in Table 5. It can be noticed that the predicted values based on Eq. 17 differ from the measured values. Equation 18 results in a too high velocity for all measurements when using the sound speed of 6800 m/s for gypsum (Table 1). When using 4571 m/s as sound velocity of gypsum as given by Dalui et al. [17], the measurements for the first two experiments show good agreement. But the values for the mixtures with higher water/binder ratio (e.g. higher void fraction) are too low. Both Eqs. 19 and 20 lead to an overestimation compared with the experimental value.

The predicted values based on Eq. 21 are close to the experimental values for all water/binder ratios. For the lowest water/binder ratios, the predictions are too low, while for the higher water/binder ratios the prediction tends to overestimate the velocity. The best results for Eq. 21 are found with the solid sound velocity of 6800 m/s.

Conclusions

The model given by Robeyst et al. [1] for predicting the sound velocity of an air–water–solids slurry is compatible with the experiments assuming a constant air content of 2.7% (V/V) based on the volume of hemihydrate. In case of the hardened (porous) material, the closest fit between experimental and predicted value is found by the use of the direct method. The best results were obtained with the series arrangement based on the empirical sound velocity values; Eq. 21 with $c_s = 6800$ m/s and $c_f = 1497$. Also the equation of Dalui et al. [17] (Eq. 18) shows a good agreement for the two lowest void fractions, using with $c_s = 4571$ m/s and $n = 0.84$.

Analysis of measurements using the hydration model

In the previous section, the ultrasonic measurements were compared with the prediction based on theoretical equations for initial and final state of the hydration. The next step is to apply the described models from 'Hydration models' section on the measured hydration curves from 'Experiments' section.

Analysis

The sound velocity graphs contain a series of characteristic important points. For instance, $t_{\alpha=0}$ is the point in time at which the sound velocity starts to increase. The time until this point is called the induction time. The previous section showed that the sound velocity of this point can be best described based with model of Robeyst (Eqs. 3–5). And $t_{\alpha=1}$ is the moment in time at which hydration is completed. The previous section showed that this could be best described by equation given by Ye (Eq. 21). These points

can be directly related to the parameters of the Schiller model. K_0 is equal to $t_{\alpha=0}$ and $K_0 + K_1 + K_2$ equals to $t_{\alpha=1}$, see Eq. 32. Figure 5 shows both points in time for wbr = 0.80.

The exact determination of the value of $t_{\alpha=1}$ is challenging, since it requires that the moment of full hydration is clearly visible in the sound velocity graphs. Since this is not really the case, another method is applied here. In this method, the time ($t_{\alpha=0.5}$) needed to perform half of the hydration ($\alpha = 0.5$) is determined. Based on Eq. 31, the sound velocity describing half hydration equals the average of the sound velocity of slurry and of hardened product. Table 6 and Fig. 6a show the determined values for $t_{\alpha=0.5}$, based on the sound velocity curves.

In order to determine the individual values of K_0, K_1 and K_2, the model is fitted to the experimental sound velocity curves taking into account the already determined values for $t_{\alpha=0.5}$. The fitting is performed using $t_{\alpha=0.5}$ of the Schiller model (Eq. 32):

$$t_{\alpha=0.5} = K_1\sqrt[3]{0.5} + K_2(1 - \sqrt[3]{1-0.5}) + K_0 = (K_1 - K_2)\sqrt[3]{0.5} + K_2 + K_0. \quad (33)$$

Table 6 and Fig. 6b show the results of the fitting. From Fig. 6a, one can notice that the total time of hydration ($t_{\alpha=1.0}$) increased with an increasing volume fraction of water in the mix. Both K_1 and K_2 seem linearly related to the volume fraction water, but these fits are not really conclusive. Ignoring the results of wbr = 1.59, there is a more clear trend visible. When doing this, K_0 and K_1 are related to the volume fraction water, while K_2 is unrelated to this property. The omission of outlier wbr = 1.59 makes sense because the sound speed of the mixture is not in line with the rest of the measurements, as well as the position of the sound velocity curve.

The current research reveals the presence and magnitude of induction times (K_0 or $t_{\alpha=0}$), while Schiller [6] neglects the induction time when applying his model. When comparing the derived value of K_1 and K_2 with the values given by Schiller [6] and Beretka and van der Touw [30], one can notice that here the values for K_1 and K_2 are lower. The lower values compared to literature [6, 30, 31] can be explained by the fact that these values were most probably

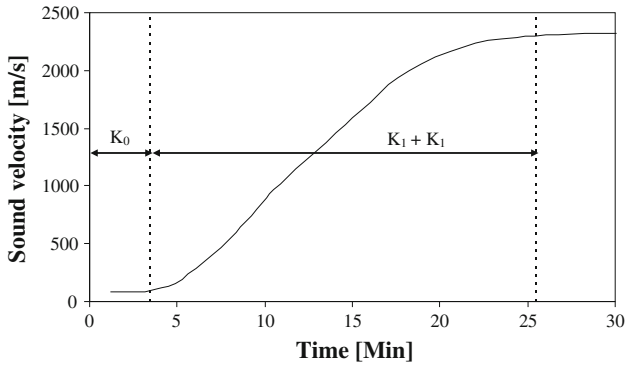

Fig. 5 Determination of K_0 and $K_1 + K_2$ for experimental results with wbr = 0.80

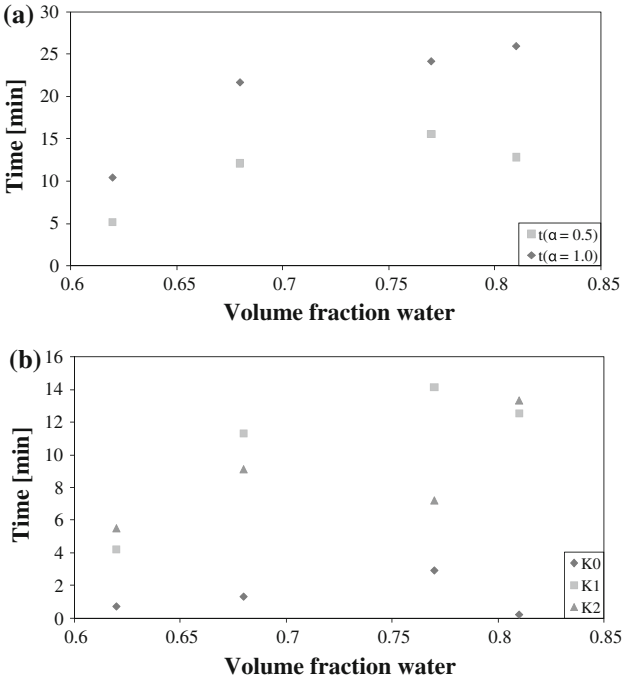

Fig. 6 **a** Determined values of $t_{\alpha=0.5}$ and $t_{\alpha=1}$ ($K_0 + K_1 + K_2$) versus the initial volume fraction of water. **b** Derived values of K_0 ($t_{\alpha=0}$), K_1 and K_2 by fitting of the experimental and simulated sound velocity curves without accelerator

Table 6 Determined value for $t_{\alpha=0.5}$ and derived values for K_1 and K_2 by fitting

Mix	wbr	Initial calculated water fraction ϕ_w	Initial calculated solid fraction ϕ_{HH}	$t_{\alpha=0.5}$	K_0	K_1	K_2	$t_{\alpha=1}$
A	0.65	0.62	0.38	5.16	0.7	4.2	5.5	10.4
B	0.8	0.68	0.32	12.14	1.3	11.3	9.1	21.7
C	1.25	0.77	0.23	15.60	2.9	14.1	7.2	24.2
D	1.59	0.81	0.19	12.86	0.2	12.5	13.3	26.0
E	1.59[acc]	0.81	0.19	9.52	2.2	6.1	12.0	20.3

[acc] stands for 0.40% m/m accelerator added

determined for α-hemihydrate. Since β-hemihydrate hydrates faster because of its larger surface area, it provides more nucleation sites for the crystallization of dihydrate [32]. The nucleation of gypsum is, according to the model of Schiller, governed by K_1.

Literature does not provide additional information describing the effect of water/binder ratio on K_1 and K_2, neither for α- nor β-hemihydrate. A research on the hydration of calcium aluminate cement using the Schiller model by Smith et al. [23] showed a relation between K_1 and water binder ratio, while the value of K_2 was constant within small water/binder ratio range. The current research shows partly the same positive relation between K_1 and water/binder ratio, particularly if the measurement with water/binder ratio of 1.59 is omitted. Furthermore, also here a relatively constant value of K_2 is observed.

Conclusions

It is shown that the relation between hydration degree and sound velocity as given by Smith et al. [23] is applicable for the hydration of hemihydrate. Within this model, the equations of Robeyst et al. [1] and Ye [18] can be used to describe the sound velocity at the start and end, respectively, of the hydration process.

Furthermore, the hydration model of Schiller is applied on the ultrasonic sound velocity measurements. A fitting of the Schiller [6] model to the experimental results has been performed using the $t_{\alpha=0.5}$ method. The analysis of the results showed that K_0 and K_1 are linearly dependent on the water/binder ratio, while K_2 is unrelated to the water/binder ratio. K_0, K_1 and K_2 describe the induction time, the dihydrate growth and the hemihydrates dissolution, respectively. Furthermore, it is noticed that the induction time ($t_{\alpha=0}$ or K_0) is linearly related to the volume fraction water and, therefore, directly related to the water/binder ratio.

Alternative method

In the previous sections, the sound speed through porous media was predicted based on the calculated void fraction. In this section, the void fraction and density are calculated based on the measured sound velocity through a porous hardened material. Equations 18 and 21 can be rewritten as

$$\phi_t = 1 - \left(\frac{c_e}{c_s}\right)^{\frac{1}{n}} = 1 - \left(\frac{c_e}{c_s}\right)^{\frac{1}{0.84}} \tag{34}$$

or

$$\phi_t = \left(\frac{c_f c_s}{c_e} - c_f\right) \cdot \frac{1}{c_s - c_f}, \tag{35}$$

respectively, with c_e is the measured sound velocity during experiments (Table 3), c_s the sound velocity through non-porous material and c_f the sound velocity through the fluid in the pores (Table 1). Table 7 shows the derived void fractions for gypsum based on Eqs. 34 and 35 using the experimental values from 'Experiments' section.

The results of Eq. 34 show that better results are obtained with a sound velocity of 4571 m/s compared to solid sound velocity of 6800 m/s. This finding is in line with 'Experiments' section, which also showed better results with a solid sound velocity of 4571 m/s. The results show a very close fit between the derived void fraction from Eq. 35 and the void fractions from model of Brouwers [19], governed by the water/binder ratio. The difference between model and derived value is limited except for wbr = 1.59 without accelerator.

The derived void fraction could be useful for deriving the density of gypsum-based materials, since the commonly used method for the determination of density of building materials is not suitable. This method included the measuring of the mass when the sample is submersed in water. Since gypsum is soluble in water, this could lead to changes in the material. The equation for the density of gypsum based on the (derived) void fraction reads

$$\rho_e = \phi_t \rho_f + (1 - \phi_t)\rho_s \tag{36}$$

with ρ_e as the apparent density, ϕ_t the void fraction, ρ_f and ρ_s the specific density of the fluid and the solid, respectively. When combining Eq. 36 with Eqs. 34 and 35, one can obtain the following equations for the effective density of the gypsum (e.g. applied in plasterboard) based on the measured effective sound velocity

Table 7 Derived void fractions based on measured sound velocity and Eqs. 34, 35

Mix	Calculated final void fraction [19]	Prediction void fraction Eq. 34 c_s = 6800 m/s	Prediction void fraction Eq. 34 c_s = 4571 m/s	Prediction void fraction Eq. 35
A	0.493	0.696	0.512	0.485
B	0.566	0.724	0.558	0.552
C	0.685	0.767	0.626	0.677
D	0.740	0.596	0.352	0.323
E	0.740	0.789	0.662	0.764

$$\rho_e = \rho_f + (\rho_s - \rho_f) \cdot \left(\frac{c_e}{c_s}\right)^{\frac{1}{0.84}} \quad (37)$$

and

$$\rho_e = \rho_s - \frac{\rho_s - \rho_f}{c_s - c_f} \cdot \left(\frac{c_f c_s}{c_e} - c_f\right), \quad (38)$$

respectively. Summarizing, based on the measured sound velocity both void fraction and apparent density can be predicted.

Conclusions

In the current article, three situations were distinguished; slurry (starting situation), hardened product (end situation) and material during hydration (situation in between slurry and hardened product). The following main findings with regard to these situations were found:

- The model of Robeyst et al. [1] for the sound velocity of a slurry showed a good agreement with the experimental values, when taking into account an air content of 2.7% (V/V) on applied hemi-hydrate.
- A very good agreement for porous hardened materials was found between the experimental and theoretical values with the series arrangement according to Ye [18] (Eq. 21) with $c_s = 6800$ m/s for dihydrate.
- The ultrasonic sound velocity through the hydrating material, which is related to the hydration curve, can be described using the combination of the hydration model of Schiller [6] and the relation between hydration degree and sound velocity given by Smith et al. [23].

Furthermore, the analysis of the results of the fitting with the Schiller model showed that the parameters K_0 (induction time) and K_1 (gypsum growth) are positively linearly related to the water/binder ratio. The parameter K_2 (dissolution of hemihydrate) is unrelated to the volume fraction water.

Acknowledgements The authors wish to express their sincere thanks to Prof. Dr.-Ing. habil. C.S. Grosse and Dipl.-Ing. F. Lehmann of Non-destructive Testing Lab, Technical University of Munich, Germany, for performing the ultrasonic tests, the European Commission (I-SSB Project, Proposal No. 026661-2) and the following sponsors of the research group: Bouwdienst Rijkswaterstaat, Graniet-Import Benelux, Kijlstra Betonmortel, Struyk Verwo, Insulinde, Enci, Provincie Overijssel, Rijkswaterstaat Directie Zeeland, A&G Maasvlakte, BTE, Alvon Bouwsystemen, V.d. Bosch Beton, Selor, Twee "R" Recyling, GMB, Schenk Concrete Consultancy, De Mobiele Fabriek, Creative Match, Intron, Geochem Research and Icopal (chronological order of joining).

References

1. Robeyst N, Gruyaert E, Grosse CU, De Belie ND (2008) Cem Concr Res 38(10):1169
2. Reinhardt HW, Grosse CU (2004) Constr Build Mater 18(3):145
3. De Belie ND, Grosse CU, Kurz J, Reinhardt HW (2005) Cem Concr Res 35(11):2087
4. Ylmén R, Jäglid U, Steenari B-M, Panas I (2009) Cem Concr Res 39(5):433
5. Reinhardt HW, Grosse CU, Herb A, Weiler B, Schmidt G. Verfahren zur Untersuchung eines erstarrenden und/oder erhärtenden Werkstoffs mittels Ultraschall, U.S. Patent 198 56 259.41999
6. Schiller K (1974) J Appl Chem Biotechnol 24(7):379
7. Sayers CM, Dahlin A (1993) Adv Cem Based Mater 1(1):12
8. Robeyst N, Grosse CU, De Belie N (2009) Cem Concr Res 39(10):868
9. Losso M, Viveiros E (2005) Sound insulation of gypsum board in practice. Presented at the 2005 Congress and Exposition on Noise Control Engineering, Rio de Janeiro, Brazil, 2005
10. Harker AH, Temple JAG (1988) J Phys D 21(11):1576
11. Austin JC, Holmes AK, Tebbutt JS, Challis RE (1996) Ultrasonics 34(2–5):369
12. Gómez Álvarez-Arenas TE, Elvira Segura L, Riera Franco de Sarabia E (2002) Ultrasonics 39(10):715
13. Hoyos M, Bacri JC, Martin J, Salin D (1994) Phys Fluids 6(12):3809
14. Landau L (1986) Theory of elasticity, 3rd edn. Pergamon Press, Oxford
15. Arnold M, Boccaccini AR, Ondracek G (1996) J Mater Sci 31(6):1643. doi:10.1007/BF00357876
16. Roth DJ, Stang DB, Swickard SM, DeGuire MR (1990) Review and statistical analysis of the ultrasonic velocity method for estimating the porosity fraction in polycrystalline materials. NASA, Cleveland, OH
17. Dalui SK, Roychowdhury M, Phani KK (1996) J Mater Sci 31(5):1261. doi:10.1007/BF00353105
18. Ye G (2003) Experimental study and numerical simulation of the development of the microstructure and permeability of cementious materials. PhD-Thesis, Delft University of Technology, The Netherlands
19. Brouwers HJH (2011) A hydration model of Portland cement using the work of Powers and Brownyard. Portland Cement Association, Skokie, IL
20. Schiller KK (1958) In: Walton WH (ed) Mechanical properties of non-brittle materials. Butterworths Sci Pub, London, pp 35–49
21. Phani KK, Niyogi SK, Maitra AK, Roychaudhury M (1986) J Mater Sci 21(12):4335. doi:10.1007/BF01106552
22. Yu QL, Brouwers HJH (2011) Constr Build Mater 25(7):3149
23. Smith A, Chotard T, Gimet-Breart N, Fargeot D (2002) J Eur Ceram Soc 22(12):1947
24. Schiller K (1962) J Appl Chem 12(3):135
25. Schiller K (1963) J Appl Chem 13(12):572
26. Schiller K (1965) Nature 205:1208
27. Ridge MJ, Surkevicius H (1961) J Appl Chem 11(11):420
28. Ridge MJ, Surkevicius H (1962) J Appl Chem 12(6):246
29. Ridge MJ, Surkevicius H (1966) J Appl Chem 16(3):78
30. Beretka J, van der Touw JW (1989) J Chem Technol Biotechnol 44(1):19
31. Fujii K, Kondo W (1986) J Chem Soc Dalton Trans 4:729
32. Singh NB, Middendorf B (2007) Prog Cryst Growth Charact Mater 53(1):57
33. Hunger M, Brouwers HJH (2009) Cem Concr Compos 31(1):39
34. Hunger M (2010) An integral design concept for ecological self-compacting concrete. PhD Thesis, Eindhoven University of Technology, Eindhoven, The Netherlands

35. Grosse U, Lehmann F (2008) Ultrasound measurements of the hydration rate of hemihydrates. Materialprufungsanstalt, Universitat Stuttgart, Stuttgart, Germany
36. Lide DR (2003) CRC handbook of chemistry and physics, 84th edn. CRC Press, Boca Raton, FL
37. Schofield PF, Stretton IC, Knight KS, Hull S (1997) Physica B 234–236:942
38. Meille S, Garboczi EJ (2001) Model Simul Mater Sci Eng 9(5):371
39. Haecker CJ et al (2005) Cem Concr Res 35(10):1948